

The Consequences of Gamma-ray Burst Jet Opening Angle Evolution on the Inferred Star Formation Rate

Nicole M. Lloyd-Ronning,^{1,2*} Jarrett L. Johnson,¹ Aycin Aykutaalp,¹

¹Los Alamos National Lab, Los Alamos, NM, USA 87545

²Department of Math, Engineering, & Science, University of New Mexico, 4000 University Dr., Los Alamos, NM, USA 87544

17 August 2021

ABSTRACT

Gamma-ray burst (GRB) data suggest that the jets from GRBs in the high redshift universe are more narrowly collimated than those at lower redshifts. This implies that we detect relatively fewer long GRB progenitor systems (i.e. massive stars) at high redshifts, because a greater fraction of GRBs have their jets pointed away from us. As a result, estimates of the star formation rate (from the GRB rate) at high redshifts may be diminished if this effect is not taken into account. In this paper, we estimate the star formation rate (SFR) using the observed GRB rate, accounting for an evolving jet opening angle. *We find that the SFR in the early universe ($z > 3$) can be up to an order of magnitude higher than the canonical estimates*, depending on the severity of beaming angle evolution and the fraction of stars that make long gamma-ray bursts. Additionally, we find an excess in the SFR at low redshifts, although this lessens when accounting for evolution of the beaming angle. Finally, under the assumption that GRBs do in fact trace canonical forms of the cosmic SFR, we constrain the resulting fraction of stars that must produce GRBs, again accounting for jet beaming-angle evolution. We find this assumption suggests a high fraction of stars in the early universe producing GRBs - a result that may, in fact, support our initial assertion that GRBs *do not* trace canonical estimates of the SFR.

Key words: stars(general)–gamma-ray bursts; cosmology

1 INTRODUCTION

Understanding the global star formation rate (SFR) density is a key factor in understanding galaxy formation and evolution throughout the history of our Universe; additionally, it provides a cosmic census of the many diverse astronomical objects in our Universe (e.g., see Hopkins & Beacom (2006); Kennicutt & Evans (2012); Krumholz (2014); Madau & Dickinson (2014) and references therein). However, accurately determining the cosmological SFR is difficult for a number of reasons. Many of these issues have to do with the assumptions invoked when trying to connect observations to a physical star formation rate density, as well as accurately accounting for observational selection effects (see, e.g., Hopkins & Beacom (2006); Madau & Dickinson (2014) for a discussion of these issues). Furthermore, observations themselves are limited - classic techniques using ultraviolet and far infrared measurements of galaxies are difficult at high redshifts; to get an accurate measurement of the star formation rate beyond a redshift of 3 or so, multiple techniques must be employed.

Because long gamma-ray bursts (LGRBs) are the most luminous explosions in the universe and because of definitive

evidence of their association with massive star progenitors (Galama et al. 1998; Hjorth et al. 2003; Woosley & Bloom 2006; Hjorth & Bloom 2012), they have long been suggested as tools with which to estimate the high redshift star formation rate (Lloyd-Ronning et al. 2002; Jakobsson et al. 2005; Kistler et al. 2008; Yüksel et al. 2008; Kistler et al. 2009; Wanderman & Piran 2010; Robertson & Ellis 2012; Trenti et al. 2013; Lien et al. 2014; Petrosian et al. 2015; Chary et al. 2016; Le & Mehta 2017; Kinugawa et al. 2019; Elías-Chávez & Martínez 2020). However, there are a number of issues that make doing so difficult, essentially related to understanding exactly what types of stars and/or fractions of the global stellar population produce GRBs (including accounting for multiple GRB progenitors), and understanding how this relationship may change over cosmic time. In addition, the distribution of the GRB beaming angle plays an important role in relating the GRB rate to the SFR. And - finally and importantly - observational selection effects in the detection of high redshift GRBs must be taken into account.

Recently, Lloyd-Ronning et al. (2019b, 2020) examined a large sample of LGRBs with redshifts (z , in the range $0.1 \lesssim z \lesssim 5$) and found that the estimates of the jet opening angle, θ_j , appear to be narrower at high redshifts than at low redshifts, with a best-fit

* E-mail: lloyd-ronning@lanl.gov

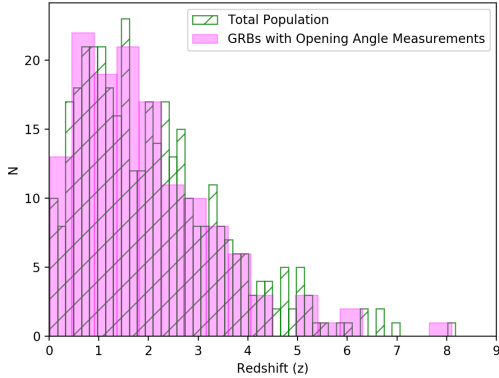


Figure 1. Redshift distribution of GRBs with jet opening angle distributions (magenta) compared to the entire population. There is no statistically significant difference between the shapes of the two distributions.

functional form of $\theta_j \propto (1+z)^{-0.8 \pm 0.2}$ (we chose a power-law fit as a straightforward way to quantify this relationship and its scatter). Lloyd-Ronning et al. (2020) argue that this may be a result of lower metallicity, higher mass (and therefore denser) stars at high redshifts collimating the GRB jet more, compared to less dense stars at lower redshifts. Several recent studies support this framework – e.g., Klencki et al. (2020) show that low metallicity leads to more compact stars, while Chruslinska et al. (2020) show a higher rate of metal-poor star formation at high redshift, leading to a top-heavy IMF. Sharda et al. (2020) show that the presence of magnetic fields can suppress fragmentation in the early universe, leading to a top-heavy IMF at higher redshifts. Additionally, low metallicity stars at high redshifts undergo less mass (and angular momentum) loss, and therefore may rotate more rapidly. This may have an effect on the jet collimation, potentially leading to more collimated jets at high redshift (for example, for a magnetically launched jet (Blandford & Znajek 1977), the angular momentum and magnetic field of the central engine may play a role in the degree of collimation of the jet (Hurtado, in prep)).

Regardless of the physical origin of the jet angle-redshift anti-correlation, a consequence of this relationship is that there exists a smaller fraction of *observable* GRB jets at high redshift, compared to those at lower redshifts. In other words, because of the narrower collimation at high redshifts, there will be a higher fraction of GRBs with jets pointed away from Earth. This leads to a higher density of GRB progenitors at high redshift than we would infer if we use a constant, non-evolving jet opening angle. This effect must be taken into account when using GRBs to estimate the high redshift star formation rate.

To estimate the star formation rate from the GRB rate, one must assume something about the fraction of stars that produce GRBs, and whether this fraction evolves through cosmic time (e.g. see Kistler et al. (2008); Yüksel et al. (2008); Kistler et al. (2009) for a straightforward summary of this issue). Alternatively, one can assume a one-to-one correspondence between the GRB rate and the SFR measured by other techniques, and then infer the fraction of stars that produce GRBs. Once again, GRB jet beaming angle evolution will affect this result and must be accounted for.

In this paper, we examine both approaches with the novel addition of accounting for beaming angle evolution through cosmic time. Our aim is twofold: 1) assuming the fraction of stars that produce IGRBs, *estimate the star formation rate* from the GRB rate

accounting for the fact that IGRB beaming angle appears to evolve with redshift, and 2) under the assumption that IGRBs trace previously determined parameterizations of the global star formation rate, *estimate the fraction of stars that must produce IGRBs* in order to be consistent with the GRB rate (again, accounting for jet beaming angle evolution).

Our paper is organized as follows. In §2, we summarize the data sample and results of Lloyd-Ronning et al. (2019b, 2020), who showed IGRBs appear to exhibit cosmic beaming angle evolution, with higher redshift IGRBs more narrowly beamed than low redshift ones. In §3, we describe the method used to estimate the star formation rate and/or fraction of stars that are progenitors for IGRBs, based on the methods described in Kistler et al. (2008); Yüksel et al. (2008); Kistler et al. (2009), and present our results. We show that IGRB beaming angle evolution leads to a star formation rate at high redshifts that is higher than canonical estimates (Madau & Dickinson 2014) for both a constant and evolving fraction of stars that produce GRBs. Alternatively, under the assumption that the IGRB rate density follows the Madau & Dickinson (2014) star formation rate density, we calculate the *inferred* fraction of stars that make GRBs (and its evolution). These results indicate that a higher fraction of stars produce GRBs at both low ($(1+z) < 3$) and high ($(1+z) > 3$) redshifts relative to the peak of star formation – a counter-intuitive result that we argue may emphasize the inaccuracy of assuming that GRBs trace the global SFR. Our conclusions are summarized in §4.

2 DATA

Our data sample is described in detail in Lloyd-Ronning et al. (2019b) and Lloyd-Ronning et al. (2020), who use data compiled in Wang et al. (2020); this latter reference contains all publicly available observations of 6289 gamma-ray bursts from 1991 to 2016. For the 376 GRBs with redshifts (and therefore isotropic energy) estimates, Lloyd-Ronning et al. (2019b) found that certain intrinsic long gamma-ray burst (IGRB) properties appear to evolve with redshift, even when accounting for Malmquist-type biases and selection effects in the observed data. However, in the hundred or so bursts where jet opening angle estimates are available and for which one can compute beaming angle corrected (that is, the actual emitted) gamma-ray energy and luminosity, Lloyd-Ronning et al. (2019b) found these variables (i.e. gamma-ray luminosity and emitted energy) are *not* correlated with redshift. This suggests that jet opening angle *is*, and indeed they found a significant anti-correlation between jet opening angle and redshift, with a functional form $\theta_j \propto (1+z)^{-0.8 \pm 0.2}$. Such an anti-correlation between jet angle and redshift was originally suggested in Lloyd-Ronning et al. (2002) (e.g. see their section 5.1.2; they suggested the faster rotation of stars at high redshift could be consistent with lower mass (and angular momentum) loss due to lower metallicity). Observational evidence for this anti-correlation has also been put forth by Lü et al. (2012) and Laskar et al. (2014, 2018a,b). An explanation for this correlation in terms of collimation by a massive star stellar envelope is given in Lloyd-Ronning et al. (2020).

2.1 The Role of Selection Effects

As mentioned above, the analysis of Lloyd-Ronning et al. (2019b) accounts for gamma-ray flux-limit selection effects in the data. However, we might ask what other types of selection effects could potentially contribute to the $\theta_j - (1+z)$ anti-correlation. In this case,

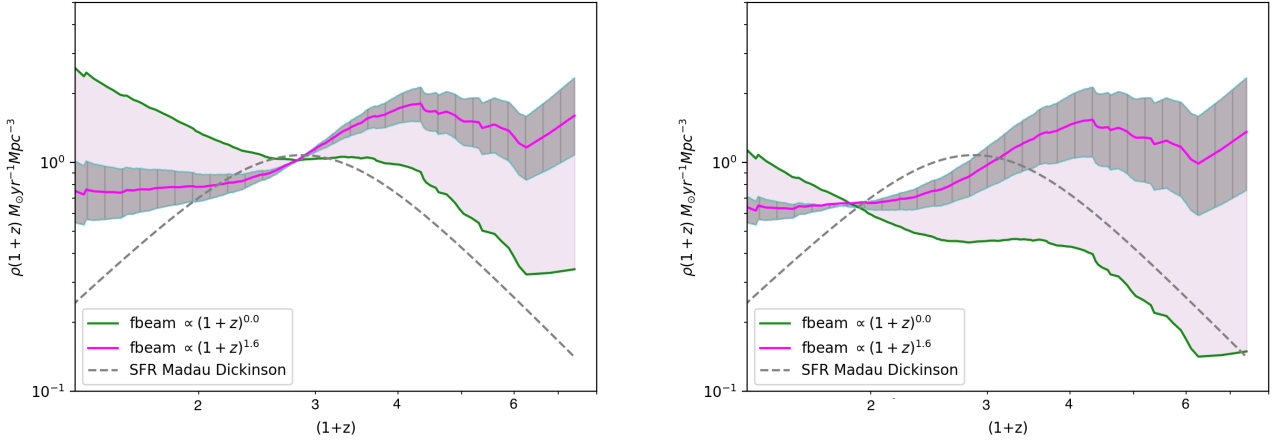


Figure 2. **Left Panel:** Star formation rate density $\rho(1+z)$ as a function of redshift $(1+z)$ assuming a constant fraction of stars produce GRBs, and accounting for beaming angle evolution, according to the best fit to the data, $\theta_j \propto (1+z)^{-0.8 \pm 0.2}$ (with the gray region denoting the error on the fit). The green line shows the inferred SFR assuming no beaming angle evolution. Curves are normalized to the MD14 star formation rate at a peak at $(1+z) = 3$. **Right Panel:** Same as left panel but curves are normalized to the MD14 star formation rate at a redshift $(1+z) = 2$.

it is important to consider jet opening angle estimate techniques and whether there is a selection against higher opening angles at larger redshifts. Indeed since opening angles are measured by breaks in afterglow light curves, when the relativistic beaming angle $1/\Gamma$ reaches the physical “edge” of the jet, larger opening angles cannot be detected until later times (for a given Γ for the outflow) and the afterglow may have faded below detector sensitivity by that point.

We have explored these issues in [Lloyd-Ronning et al. \(2019b, 2020\)](#) (see also the recent paper by [Le et al. \(2020\)](#) who look at biases in redshift distributions and jet opening angles between different subsets of GRB data.). In particular, in [Lloyd-Ronning et al. \(2020\)](#) we implemented a strong artificial truncation in the $\theta_j - (1+z)$ plane, which mimics a selection against large opening angles at high redshifts. Even when accounting for this selection bias using established non-parametric statistical techniques ([Efron & Petrosian 1992; Efron & Petrosian 1999](#)), we find there is still a significant anti-correlation between θ_j and $(1+z)$. We also note that the redshift distribution of GRBs with jet opening angle estimates is not different from that of the entire sample of GRBs. A Kolmogorov-Smirnov (KS) test comparing the two distributions gives a p value of 0.64 that they are drawn from the same parent distribution - in other words, the redshift distributions of GRBs with jet opening angle measurements and the entire sample of GRBs are statistically the same (histograms of the two samples are shown in [Figure 1](#)). Because there is roughly same relative fraction of jet opening angle measurements at low and high redshifts ($\sim 1/3$), this suggests we may not be missing a large fraction of large opening angle GRBs at high redshift and that the anti-correlation between jet opening angle and redshift may indeed have a physical origin.

In what follows, we assume the jet opening angle-redshift anti-correlation is physical, and explore how this relationship can affect estimates of the high redshift star formation rate.

3 RESULTS

Because of the strong evidence that IGRBs are associated with the deaths of massive stars (e.g. see [Woosley & Bloom \(2006\); Hjorth &](#)

[Bloom \(2012\)](#) for summaries), and because they are so luminous and can be detected to such high redshifts, many authors have attempted to use GRBs to estimate the high redshift star formation rate ([Lloyd-Ronning et al. 2002; Kistler et al. 2008; Yüksel et al. 2008; Kistler et al. 2009; Wanderman & Piran 2010; Robertson & Ellis 2012; Trenti et al. 2013; Lien et al. 2014; Petrosian et al. 2015; Kinugawa et al. 2019](#)). However, as mentioned in the introduction, there are a number of complicating issues in understanding exactly how IGRBs track or trace the global star formation rate. One must address a host of issues in accurately determining the IGRB rate - flux sensitivity selection effects and other observational biases must be accounted for (e.g. [Lloyd-Ronning et al. \(2002\); Petrosian et al. \(2015\); Lloyd-Ronning et al. \(2019b\)](#)) to get an accurate measure of the true, underlying IGRB rate. Additionally, because we will in general only observe a fraction $d\Omega/4\pi$ of those GRBs whose jets are directed toward us (where $d\Omega = 2\pi(1 - \cos(\theta_j))$ is the jet solid angle), an understanding of the behavior of GRB beaming angle distribution is necessary to correct for the true underlying number of GRB progenitor systems. Finally, we need to get a handle on the GRB progenitor system - exactly what fraction of stars make long gamma-ray bursts, and how does this fraction evolve as a function of redshift?

3.1 Obtaining the Star Formation Rate from the IGRB Rate

There are several possible approaches to tackling this problem. One straightforward approach is laid out in [Kistler et al. \(2008\); Yüksel et al. \(2008\); Kistler et al. \(2009\)](#). One can essentially parameterize the various unknowns mentioned above to estimate the star formation rate from the IGRB rate:

$$\dot{\rho}_{\text{SFR}}(z) = \left(\frac{dN}{dz}\right) (f_{\text{beam}}(z)) \left(\frac{(1+z)}{dV/dz}\right) \frac{1}{\epsilon(z)} \quad (1)$$

where dN/dz is the true, underlying IGRB rate (accounting for the GRB luminosity function and detector trigger selection effects), $\epsilon(z)$ parameterizes the fraction of stars that make GRBs (and in

principle can evolve with redshift), and $f_{beam}(z)$ is a factor (> 1) that accounts for the number of GRBs missed due to beaming. The factor dV/dz is the cosmological volume element given by:

$$dV/dz = 4\pi \left(\frac{c}{H_o} \right)^3 \left[\int_1^{1+z} \frac{d(1+z)}{\sqrt{\Omega_\Lambda + \Omega_m(1+z)^3}} \right]^2 \times \frac{1}{\sqrt{\Omega_\Lambda + \Omega_m(1+z)^3}} \quad (2)$$

where we use $\Omega_m = 0.286$, an $\Omega_\Lambda = 0.714$ and an $H_o = 69.6 \text{ km s}^{-1} \text{ Mpc}^{-1}$. [Lloyd-Ronning et al. \(2019b\)](#) describe how they obtained the differential rate distribution of long GRBs as a function of redshift, dN/dz , using the non-parameteric methods of [Lynden-Bell \(1971\)](#); [Efron & Petrosian \(1992\)](#); [Efron & Petrosian \(1999\)](#). In particular, this quantity reflects the underlying GRB rate distribution, accounting for observational selection effects. We refer the reader to [Lloyd-Ronning et al. \(2019b\)](#) for a discussion of how this distribution is obtained. The factor we focus on here is $f_{beam}(z)$. In previous studies, this was assumed to be a constant. The results of [Lloyd-Ronning et al. \(2019b, 2020\)](#), however, suggest that this function evolves with redshift. This factor - a number greater than one, which parameterizes the number of GRBs missed due to jets being pointed away from us - is proportional to the inverse of the solid angle of the jet. Therefore, because the solid angle is proportional to θ_j^2 for small jet opening angles, if the jet opening angle θ_j evolves as $(1+z)^{-\alpha}$, the function $f_{beam} \propto (1/\theta_j^2) \propto (1+z)^{2\alpha}$.

[Lloyd-Ronning et al. \(2019b\)](#) found $\alpha \sim 0.8$, which leads to $f_{beam}(z) \propto (1+z)^{1.6}$. [Figure 2](#) shows the star formation rate derived from equation 1 above, given the functional form of beaming angle evolution seen in the data (magenta line, with the error indicated by the gray region). Here we have assumed that the fraction of stars $\epsilon(z)$, that produce IGRBs remains relatively constant throughout cosmic time. The green line in this figure shows the inferred SFR assuming no beaming angle evolution (but still a constant $\epsilon(z)$). As expected, if IGRBs are more narrowly beamed in the high redshift universe, then - for a given fraction of stars that make IGRBs - there is a relatively higher star formation rate in the early universe.

Because of the uncertainties in associating the IGRB rate with the global star formation rate, there is some freedom in how to normalize our star formation rate curves in [Figure 2](#). One possibility is to normalize the star formation rate derived from the IGRB rate with that of the [Madau & Dickinson \(2014\)](#) (hereafter, MD14) rate at a redshift of $(1+z) \approx 3$, where star formation appears to peak. This is shown in the left panel of [Figure 2](#). However, the star formation rate is better determined observationally at lower redshifts (see, e.g., [Figure 1](#) of [Hopkins & Beacom \(2006\)](#)), and therefore normalizing our curves to the MD14 rate at $(1+z) \approx 2$ (or even lower) is also justifiable. We show this normalization in the right panel of [Figure 2](#). Note there appears to be an excess at low redshifts (particularly when beaming angle evolution is *not* taken into account), which we discuss further in §3.3 below.

Regardless of normalization, [Figure 2](#) indicates that the shape or functional form of the SFR throughout cosmic time, as inferred from the GRB rate, is different from the MD14 rate (given a constant fraction of stars that make IGRBs). In particular, when beaming evolution is accounted for, the peak of the SFR appears at redshifts of $z \sim 3$ (or higher) and there is a higher rate of SFR in the early universe than predicted by other estimates (on which the MD14 rate is based).

Of course there is no reason to expect that the fraction of stars that make IGRBs should be constant throughout cosmic time. Given the conditions of low metallicity (and, relatedly, high angular mo-

mentum) necessary to launch a GRB jet ([MacFadyen & Woosley 1999](#); [Yoon & Langer 2005](#); [Hirschi et al. 2005](#); [Yoon et al. 2006](#); [Woosley & Heger 2006](#)), we might expect that a higher fraction of stars in the early universe make IGRBs compared to those in the lower redshift universe. How exactly to parameterize or account for this is unclear, however. In [Figure 3](#) we show the star formation rate assuming two different functions for the evolution of the fraction of stars that make GRBs: $\epsilon(z) \propto (1+z)^{0.1}$ (green curve) and $\epsilon(z) \propto (1+z)^{1.0}$ (cyan curve). In these figures, we use a beaming evolution consistent with the relationship found in [Lloyd-Ronning et al. \(2019b, 2020\)](#), $f_{beam} \propto (1+z)^{1.6}$. Our results indicate, again, that - whether or not the fraction of stars that make GRBs evolves through cosmic time - the SFR derived from the GRB rate is different from the MD14 rate, and higher at large redshifts, when beaming angle evolution is accounted for.

3.2 The High Redshift Star Formation Rate

Accounting for potential IGRB beaming angle evolution has a significant effect on the inferred high redshift star formation rate, leading to estimates that are up to an order of magnitude higher than the MD14 rate. Interestingly, the peak of the inferred SFR (even without accounting for beaming angle evolution) appears to be around $(1+z) \sim 4$, compared with $(1+z) \sim 3$ of the MD14 rate. This may be a reflection of the IGRB rate tracing the evolution of a specific progenitor (e.g. low metallicity, massive stars) rather than the global stellar population. In addition, our SFR curve is fairly flat from redshifts between $3.5 < (1+z) < 6$. A similarly flat curve was found in the analyses of [Kistler et al. \(2008\)](#); [Petrosian et al. \(2015\)](#); [Lloyd-Ronning et al. \(2019b\)](#), without accounting for beaming angle evolution (although their inferred SFRs are flat between slightly different redshift ranges).

It is possible that the IGRB rate at high redshifts more closely follows galactic nuclear star formation, leading to a different redshift peak compared to MD14 rate. For example, [Hopkins & Beacom \(2006\)](#) suggest that the accretion of gas onto central supermassive black holes, triggered by mergers and/or interactions of galaxies, leads to starbursts (and active galactic nuclei (AGN) activity). This AGN activity is expected to peak around $(1+z) \sim 4$ ([Miyaji et al. 2015](#)), closer to the peak of the SFR we derive from the IGRB rate. Indeed numerical simulations have shown that the gravitational tidal torques excited during major mergers lead to rapid inflows of gas into the centers of galaxies ([Barnes & Hernquist 1996](#)) which can be a mechanism to trigger starbursts in galaxies. In addition, [Hopkins & Quataert \(2010\)](#) find that AGN activity is more tightly coupled to nuclear star formation than the global star formation rate of a galaxy. This is also seen in numerical simulations of [Aykutalp et al. \(2014, 2019\)](#). Finally, [Hocuk & Spaans \(2010\)](#) found that in the X-ray irradiated case, fewer stars are formed but *with a higher initial masses*. Therefore, again, the IGRB rate may align more with this channel of star formation and will lead to an SFR peak that occurs earlier than the MD14 rate.

3.3 On the Excess Rate at Low Redshifts

The star formation rate we derive from the IGRB rate shows an excess at low redshifts compared to the MD14 rate. The effect is less pronounced when we account for beaming angle evolution (but still there to some extent). We note that at very low redshifts (as $(1+z) \rightarrow 1$), the volume element (e.g. equation 2) goes to zero

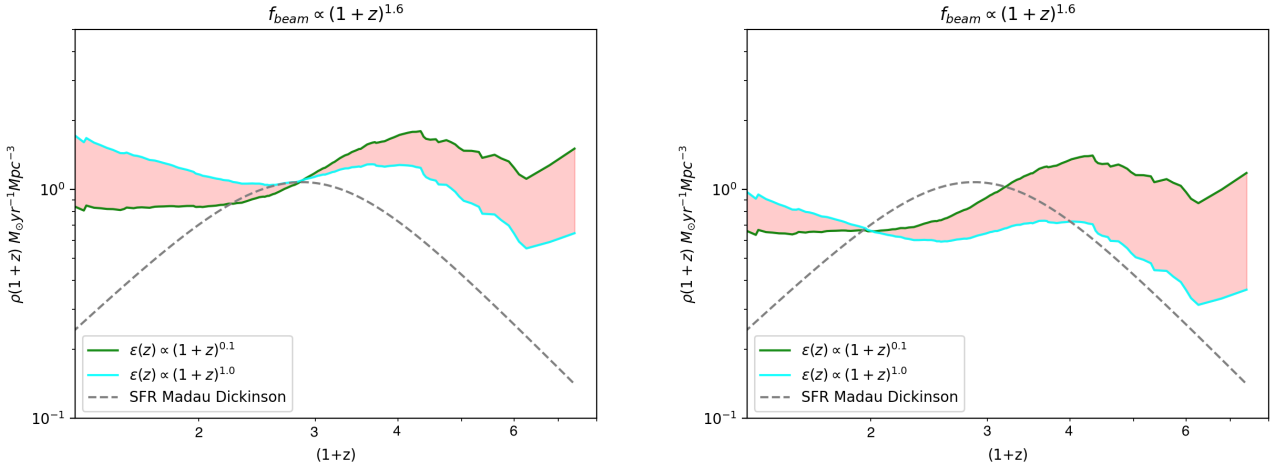


Figure 3. **Left Panel:** Star formation rate density $\rho(1+z)$ as a function of redshift $(1+z)$ assuming the fraction of stars $\epsilon(1+z)$ that produce GRBs evolves with redshift, with $\epsilon(1+z) \propto (1+z)^{0.1}$ (green line) and $\epsilon(1+z) \propto (1+z)^1$. (cyan line). We take a beaming angle evolution of $f_{beam} \propto (1+z)^{1.6}$, consistent with the anti-correlation we find in the data between jet opening angle and redshift. Curves are normalized at the peak of the MD14 SFR. **Right Panel:** Same as left panel but with the curves normalized to the MD14 star formation rate at a redshift of $(1+z) \sim 2$.

faster than the observed IGRB rate (dN/dz) does, and this causes the star formation rate in equation 1 to diverge at low redshifts. This effect comes into play around a redshift of $z \sim 0.3$; as a result, we show our results down to that limit, before the divergence becomes too severe (see also the discussion in Lloyd-Ronning et al. (2019b) of this issue).

However, even before this numerical effect comes into play, an excess at low redshifts appears to exist. This was also noted in Petrosian et al. (2015); Yu et al. (2015) and Lloyd-Ronning et al. (2019b). We emphasize that these analyses account for the greater probability of detecting low luminosity GRBs at low redshifts (i.e. Malquist biases) through non-parametric statistical techniques that account for the GRB luminosity function (although we caution a single - albeit conservative - detector flux limit was used in our analysis; in reality the detector trigger criteria are more complicated). Another approach is to impose a minimum luminosity cutoff as in Kistler et al. (2008) - this will eliminate the excess of low luminosity GRBs at small redshifts (and as a result mitigate the excess in the inferred SFR at these redshifts).

Again, this effect is more pronounced when beaming angle evolution is *not* accounted for. Therefore, it may be that beaming angle evolution is stronger than we have estimated and the low redshift star formation rate in fact roughly matches the MD14 rate at low redshifts (as in the lower part of the gray region in Figure 2) (in this case, the high redshift star formation rate is then vastly larger than that of the MD14 rate).

Another possibility for the mismatch at low redshifts could result from the array of progenitors that potentially contribute to IGRB rate (Levan et al. 2016), which may be more pronounced at low redshifts. That is, there may exist a greater number IGRB progenitor systems that are viable at lower redshifts. For example, certain binary merger systems proposed for IGRBs - which require more cosmic time to form and merge - may play a larger role in the IGRB rate at low redshifts. Additionally, they do not necessarily need the low metallicity conditions required of single star progenitors (Metha & Trenti 2020; Hao et al. 2020). Meanwhile, single star progenitors may become less viable at low redshifts due

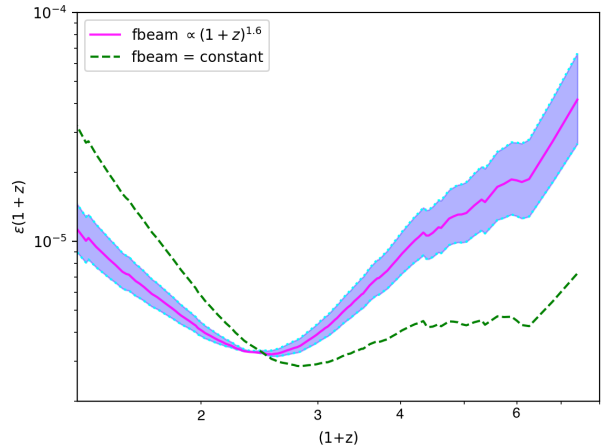


Figure 4. Fraction of stars $\epsilon(1+z)$ that make long gamma-ray bursts assuming the IGRB rate density directly traces the MD14 star formation rate density. The magenta line and purple region show this quantity accounting for jet beaming angle evolution seen in the data $\theta_j \propto (1+z)^{-0.8 \pm 0.2}$. The green dashed line shows $\epsilon(1+z)$ assuming no beaming angle evolution.

to the higher metallicity and accompanying higher mass loss (Chrimes et al. 2020; Price-Whelan et al. 2020; Klencki et al. 2020; Metha & Trenti 2020).

Finally, it may also be that the functional form of the parameterizations in equation 1 (particularly $f_{beam}(z)$ and $\epsilon(z)$) are not simple power laws, but are more complicated than what we have assumed. We argue (here and in Lloyd-Ronning et al. (2019b, 2020)) that the data are reasonably parameterized by a power-law for $f_{beam}(z)$. However, $\epsilon(z)$ could potentially be a very complicated function and indeed as we show below, when the GRB rate is assumed to follow the MD14 star formation rate, an interesting function for $\epsilon(z)$ emerges.

3.4 Estimating the Fraction of Stars Producing IGRBs

In our prescription above, we have assumed that some given fraction of stars (parameterized by the function $\epsilon(z)$) produces GRBs. However, metallicity plays a strong role in stellar evolution, affecting the stellar structure, as well as the mass and angular momentum loss of a massive star - quantities that are all crucially connected to whether or not a GRB will be successfully produced in its collapse. And because metallicity evolves through cosmic time (e.g. Pettini et al. (1997); Lara-López et al. (2009); Yuan et al. (2013)), we therefore might reasonably expect that the fraction of stars that produce GRBs will evolve with redshift, with more stars able to produce GRBs at lower metallicities (higher redshifts). This is the motivation behind our parameterizations of $\epsilon(z)$ in Figure 3, where we assumed a power-law evolution of the fraction of stars that produce GRBs. We note that an important consideration in all of this is whether the star is in a binary system, and how this (along with metallicity) plays a role in the evolving fraction of stars that produce GRBs (Metha & Trenti 2020).

Therefore, another approach we may take in using the IGRB rate to learn something about star formation history, is to assume that the IGRB rate roughly traces the MD14 functional form of the global SFR, and solve for the fraction of stars that produce IGRBs. In other words, one can take an assumed star formation rate, and - given the observed GRB rate - estimate the fraction of stars that make GRBs as a function of redshift:

$$\epsilon(z) = (d\dot{N}/dz)(f_{\text{beam}}(z)) \left(\frac{(1+z)}{dV/dz} \right) \frac{1}{\dot{\rho}_{\text{SFR}}(z)} \quad (3)$$

Where we use

$$\dot{\rho}_{\text{SFR}}(z) = .0015 \frac{(1+z)^{2.7}}{(1 + [(1+z)/2.9]^{5.6})} \text{M}_{\odot} \text{yr}^{-1} \text{Mpc}^{-3}. \quad (4)$$

for our star formation rate (Madau & Dickinson 2014).

We show this estimate for $\epsilon(z)$ in Figure 4, where the magenta line (and purple region) indicates our estimate accounting for jet opening angle evolution and the green dashed line assumes no beaming angle evolution with redshift. We choose to conservatively normalize the curves to a value of $\sim 5 \times 10^{-6}$ at a redshift of $(1+z) \sim 3$, where star formation peaks. We obtained this value by assuming roughly 0.1% of stars result in a supernova - of these supernovae, only about $\sim 15\%$ (Smith et al. 2011) are of Type Ib/c, the type associated with long gamma-ray bursts. Of this subset of Type Ib/c supernovae, only about 10% (Chapman et al. 2007; Kanaan & de Freitas Pacheco 2013) successfully launch a GRB jet (due to conditions such as sufficient angular momentum and magnetic flux to launch a jet powerful enough to pierce through the progenitor envelope; a discussion of some of these issues can be found in Lloyd-Ronning et al. (2019a)). This normalization is a big uncertainty, of course, and there is room for a range of values given our current state of knowledge.

Regardless of the normalization, we can try to understand the resulting shape of the curves in Figure 4. There is a counter-intuitively large dip in the fraction of stars that make GRBs right at the peak of star formation, when we take this approach. The increase in $\epsilon(z)$ at high redshifts may be plausible due to decreasing metallicity and possibly a top-heavy IMF at higher redshifts. The increase in $\epsilon(z)$ at lower redshifts is uncertain and may, again, be a reflection of the breakdown between single star collapse progenitors and IGRBs (see §3.3 above on the excess at low redshifts). However, ultimately, the curve we find for $\epsilon(z)$ - under the assumption that the GRB rate

traces the MD14 SFR - may be emphasizing that GRBs, in fact, do *not* trace the global star formation rate.

It is important to note, however, that the relative fraction of stars that produce IGRBs changes significantly *when accounting for beaming angle evolution of the GRB jet*. As seen in Figure 4, there is a much higher fraction of stars that make GRBs at high redshifts and relatively less at low redshift, when accounting for the change in average jet beaming angle over cosmic time. Regardless of the validity of the underlying assumption of the IGRB rate tracing the global SFR, this emphasizes the importance of accounting for jet opening angle evolution when trying to understand the relationship of IGRBs to their progenitor systems.

4 CONCLUSIONS

Observations suggest that the jet opening angles of IGRBs evolve over cosmic time, with IGRBs at higher redshifts more narrowly beamed than those at lower redshifts. In this paper we have: 1) estimated the star formation rate from the gamma-ray burst formation rate, accounting for the evolution of the distribution of GRB jet opening angles (and given an assumption about the fraction of stars that make long gamma-ray bursts), 2) estimated the fraction of stars that make long gamma-ray bursts under the assumption that IGRBs trace the global star formation rate as parameterized by MD14.

Our main results are as follows:

- When accounting for beaming angle evolution - with IGRBs more narrowly beamed at higher redshifts - we find a higher relative star formation rate at high redshifts. *Depending on the strength of the beaming angle evolution and the normalization of the inferred SFR, the SFR can be up to an order of magnitude higher than the canonical MD14 estimate.* Our inferred SFRs from the GRB rate may be indicating a specific metallicity dependent SFR (see, e.g., Björnsson (2019); Chruslinska et al. (2020)), given the low-metallicity requirements for successfully launching a GRB jet in a massive star.

- There appears to be an excess in our SFR estimates at *low redshifts* relative to the MD14 rate (again, depending on the normalization we choose). Accounting for beaming angle evolution lessens this excess, which may suggest the importance of accounting for the evolution. Alternatively, this could be a reflection of the breakdown of a one-to-one correspondence between IGRBs and massive star progenitor systems at low redshifts. In other words, if multiple systems (including binary merger systems) contribute significantly to the GRB rate at low redshifts this may lead to such an excess at low redshifts.

- Under the assumption that GRBs trace the MD14 star formation rate, we estimate the fraction of stars that produce IGRBs (in order to be consistent with the observed GRB rate), once again accounting for beaming angle evolution. Although the overall normalization of this curve is uncertain, we find that this approach implies a higher fraction of stars in the early universe produce GRBs. This result is plausible in light of the fact that low metallicity conditions are conducive to launching a successful GRB. We also find, using this approach, that a higher fraction of stars produce GRBs at lower redshifts than at the peak of star formation (although less so when beaming angle evolution is accounted for). As discussed above, this

somewhat unexpected result could reflect the breakdown of a one-to-one correspondence between IGRBs and massive star progenitors at low redshifts, and may also indicate the implausibility of assuming that the IGRB rate density follows the SFR as parameterized by MD14.

Because of the extreme luminosity of long gamma-ray bursts, they remain powerful probes of the early universe, and potentially important tools with which to measure the star formation rate at redshifts that are inaccessible by other methods. That the jet opening angle of IGRBs may evolve over cosmic time, with jets in the early universe being more narrowly beamed than those at lower redshifts, has important implications on estimates of the star formation rate from the IGRB rate - implying it has perhaps up until now been largely underestimated. As the next generation of telescopes is launched - including deep space optical and infrared probes such as the *James Webb Space Telescope* and *Nancy Grace Roman Telescope*, as well as transient detectors such as *Theseus* and the *Space Variable Objects Monitor* - we will get a more extensive probe into the early universe. In addition, new methods employing measurements of the neutrino flux (Riya & Rentala 2020), for example, could enable us to more securely ascertain star formation during these epochs, allowing us to test our predictions of the SFR at high redshift, and gain a better understanding of the history of star formation throughout our Universe.

5 ACKNOWLEDGEMENTS

We thank the referee for a very thoughtful report which led to many improvements in this manuscript. We are very grateful to John Beacom for interesting discussions, and a number of helpful comments and suggestions related to this work. We also thank Vahe' Petrosian for discussions on the rate at low redshifts. This work was supported by the US Department of Energy through the Los Alamos National Laboratory. Los Alamos National Laboratory is operated by Triad National Security, LLC, for the National Nuclear Security Administration of U.S. Department of Energy (Contract No. 89233218CNA000001). J. L. J. and A. A. are supported by a LANL LDRD Exploratory Research Grant 20170317ER. LA-UR-20-23600

6 DATA AVAILABILITY

The data underlying this article are publicly available at <https://iopscience.iop.org/article/10.3847/1538-4357/ab0a86>.

REFERENCES

- Aykutalp A., Wise J. H., Spaans M., Meijerink R., 2014, *ApJ*, **797**, 139
 Aykutalp A., Barrow K. S. S., Wise J. H., Johnson J. L., 2019, arXiv e-prints, p. arXiv:1910.08554
 Barnes J. E., Hernquist L., 1996, *ApJ*, **471**, 115
 Björnsson G., 2019, *ApJ*, **887**, 219
 Blandford R. D., Znajek R. L., 1977, *MNRAS*, **179**, 433
 Chapman R., Tanvir N. R., Priddey R. S., Levan A. J., 2007, *MNRAS*, **382**, L21
 Chary R., Petitjean P., Robertson B., Trenti M., Vangioni E., 2016, *Space Sci. Rev.*, **202**, 181
 Chrimes A. A., Stanway E. R., Eldridge J. J., 2020, *MNRAS*, **491**, 3479
 Chruslinska M., Jerabkova T., Nelemans G., Yan Z., 2020, arXiv e-prints, p. arXiv:2002.11122
 Efron B., Petrosian V., 1992, *ApJ*, **399**, 345
 Efron B., Petrosian V., 1999, *Journal of the American Statistical Association*, **94**, 824
 Elías-Chávez M., Martínez O. M., 2020, arXiv e-prints, p. arXiv:2006.03367
 Galama T. J., et al., 1998, *Nature*, **395**, 670
 Hao J.-M., Cao L., Lu Y.-J., Chu Q.-B., Fan J.-H., Yuan Y.-F., Yuan Y.-H., 2020, arXiv e-prints, p. arXiv:2005.07630
 Hirschi R., Meynet G., Maeder A., 2005, *A&A*, **443**, 581
 Hjorth J., Bloom J. S., 2012, *Gamma-ray bursts*
 Hjorth J., et al., 2003, *Nature*, **423**, 847
 Hocuk S., Spaans M., 2010, *A&A*, **522**, A24
 Hopkins A. M., Beacom J. F., 2006, *ApJ*, **651**, 142
 Hopkins P. F., Quataert E., 2010, *MNRAS*, **407**, 1529
 Jakobsson P., et al., 2005, *MNRAS*, **362**, 245
 Kanaan C., de Freitas Pacheco J. A., 2013, *A&A*, **559**, A64
 Kennicutt R. C., Evans N. J., 2012, *ARA&A*, **50**, 531
 Kinugawa T., Harikane Y., Asano K., 2019, arXiv e-prints,
 Kistler M. D., Yüksel H., Beacom J. F., Stanek K. Z., 2008, *ApJ*, **673**, L119
 Kistler M. D., Yüksel H., Beacom J. F., Hopkins A. M., Wyithe J. S. B., 2009, *ApJ*, **705**, L104
 Klencek J., Nelemans G., Istrate A., Pols O., 2020, arXiv e-prints, p. arXiv:2004.00628
 Krumholz M. R., 2014, *Phys. Rep.*, **539**, 49
 Lara-López M. A., Cepa J., Bongiovanni A., Castañeda H., Pérez García A. M., Fernández Lorenzo M., Póvic M., Sánchez-Portal M., 2009, *A&A*, **493**, L5
 Laskar T., et al., 2014, *ApJ*, **781**, 1
 Laskar T., Berger E., Chornock R., Margutti R., Fong W.-f., Zauderer B. A., 2018a, *ApJ*, **858**, 65
 Laskar T., et al., 2018b, *ApJ*, **859**, 134
 Le T., Mehta V., 2017, *ApJ*, **837**, 17
 Le T., Ratke C., Mehta V., 2020, *MNRAS*, **493**, 1479
 Levan A., Crowther P., de Grijs R., Langer N., Xu D., Yoon S.-C., 2016, *Space Sci. Rev.*, **202**, 33
 Lien A., Sakamoto T., Gehrels N., Palmer D. M., Barthelmy S. D., Graziani C., Cannizzo J. K., 2014, *ApJ*, **783**, 24
 Lloyd-Ronning N. M., Fryer C. L., Ramirez-Ruiz E., 2002, *ApJ*, **574**, 554
 Lloyd-Ronning N. M., Fryer C., Miller J. M., Prasad N., Torres C., Martin P., 2019a, *MNRAS*, **485**, 203
 Lloyd-Ronning N. M., Aykutalp A., Johnson J. L., 2019b, *MNRAS*, **488**, 5823
 Lloyd-Ronning N., Hurtado V. U., Aykutalp A., Johnson J., Ceccobello C., 2020, *MNRAS*,
 Lü J., Zou Y.-C., Lei W.-H., Zhang B., Wu Q., Wang D.-X., Liang E.-W., Lü H.-J., 2012, *The Astrophysical Journal*, **751**, 49
 Lynden-Bell D., 1971, *MNRAS*, **155**, 95
 MacFadyen A. I., Woosley S. E., 1999, *ApJ*, **524**, 262
 Madau P., Dickinson M., 2014, *ARA&A*, **52**, 415
 Metha B., Trenti M., 2020, arXiv e-prints, p. arXiv:2004.09716
 Miyaji T., et al., 2015, *ApJ*, **804**, 104
 Petrosian V., Kitandis E., Kocevski D., 2015, *ApJ*, **806**, 44
 Pettini M., Smith L. J., King D. L., Hunstead R. W., 1997, *ApJ*, **486**, 665
 Price-Whelan A. M., et al., 2020, arXiv e-prints, p. arXiv:2002.00014
 Riya Rentala V., 2020, arXiv e-prints, p. arXiv:2007.02951
 Robertson B. E., Ellis R. S., 2012, *ApJ*, **744**, 95
 Sharda P., Federrath C., Krumholz M. R., 2020, arXiv e-prints, p. arXiv:2002.11502
 Smith N., Li W., Filippenko A. V., Chornock R., 2011, *MNRAS*, **412**, 1522
 Trenti M., Perina R., Tacchella S., 2013, *ApJ*, **773**, L22
 Wanderman D., Piran T., 2010, *MNRAS*, **406**, 1944
 Wang F., Zou Y.-C., Liu F., Liao B., Liu Y., Chai Y., Xia L., 2020, *ApJ*, **893**, 77
 Woosley S., Bloom J., 2006, *Annu. Rev. Astron. Astrophys.*, **44**, 507
 Woosley S. E., Heger A., 2006, *ApJ*, **637**, 914
 Yoon S.-C., Langer N., 2005, *A&A*, **443**, 643
 Yoon S.-C., Langer N., Norman C., 2006, *A&A*, **460**, 199

8 *Lloyd-Ronning et al.*

Yu H., Wang F. Y., Dai Z. G., Cheng K. S., 2015, [ApJS](#), **218**, 13

Yuan T. T., Kewley L. J., Richard J., 2013, [ApJ](#), **763**, 9

Yüksel H., Kistler M. D., Beacom J. F., Hopkins A. M., 2008, [ApJ](#), **683**, L5

This paper has been typeset from a \TeX/L\AA\TeX file prepared by the author.